A novel solution for school renovations

Combining diffuse ceiling ventilation with double skin facade

Bugenings, Laura Annabelle; Schaffer, Markus; Larsen, Olena Kalyanova; Zhang, Chen

Published in:
Journal of Building Engineering

DOI (link to publication from Publisher):
10.1016/j.jobe.2022.104026

Publication date:
2022

Document Version
Publisher's PDF, also known as Version of record

Journal of Building Engineering 49 (2022) 104026

Contents lists available at ScienceDirect

Journal of Building Engineering

journal homepage: www.elsevier.com/locate/jobe

A novel solution for school renovations: Combining diffuse ceiling ventilation with double skin facade

Laura Annabelle Bugenings [1], Markus Schaffer, Olena Kalyanova Larsen [*], Chen Zhang

Department of the Built Environment, Aalborg University, Aalborg, 9220, Denmark

A R T I C L E I N F O

Keywords:
Double skin facade
Diffuse ceiling ventilation
Building performance simulation
Energy saving potential
School refurbishment

A B S T R A C T

With the aim to increase today's low retrofitting rate and thus decrease the currently rising energy consumption of the building sector, this work proposes a novel renovation concept for schools. Therefore, two components, double skin facade (DSF) and diffuse ceiling ventilation (DCV), are combined with an exhaust ventilation system, providing an alternative to a traditional renovation where windows are replaced, the external wall is insulated and a balanced ventilation system is installed. Further, based on a Danish case study classroom, different configurations of the novel system, with varying glazing properties and DSF cavity thicknesses are compared against a range of traditional renovations through building performance simulation using IDA-ICE. The results indicate that the new system can achieve up to 11% lower total primary energy consumption as the best traditional renovation while achieving an equal indoor environmental quality and therefore offering designers and engineers a competitive alternative for school renovation projects. Additionally, employing a sensitivity analysis, it could be demonstrated for the primary energy consumption and the global thermal comfort that the glazing (number of panes and physical properties) has a superior influence on the novel system compared to the cavity thickness.

1. Introduction

Well known is the "20-20-20" aim of the European Union (EU) (reduction of greenhouse gas by 20%, 20% energy from renewable sources, and 20% improvement in energy efficiency) and yet in 2020, with the most recent data from 2019 [2] (before the Covid-19 pandemic), it is not clear if all those targets will be met, while the prognosis for the next big goal, the 2030 targets, is even grimmer. One aspect that contributes to this is that the final energy consumption did not decrease in the five years before 2019 [2].

Two sectors mainly cause this lack of decrease in energy consumption; the transport sector with an increase of the energy

Abbreviations: ACH, air change rate per hour (h^{-1}); BPS, building performance simulation; C_d, discharge coefficient; DCV, diffuse ceiling ventilation; DSF, double skin facade; E_{ref}, energy balance for windows (kW/m^2); g, solar heat gain coefficient; HY, hysteresis; IAQ, indoor air quality; IEQ, indoor environmental quality; n, number of simulations; ORM_4, outdoor running mean temperature over 4 days including the current day; ORM_{30}, outdoor running mean temperature over the last 30 days excluding the current day; PE, primary energy; PMV, predicted mean vote; PPD, predicted precentage of dissatisfied; SFP, specific fan power ($kW/(m^3s)$); T_{air}, air temperature (°C); T_c, thermal neutral temperature (°C); T_{ext}, external air temperature (°C); T_{op}, operative temperature (°C); I_{sun}, solar irradiation on facade (W/m^2); U_f, U-value window frame ($W//m^2K$)); U_g, U-value window glazing($W//m^2K$)); VAV, variable air volume.

* Corresponding author.
E-mail address: ok@build.aau.dk (O.K. Larsen).
[1] Present address: Department of Civil and Architectural Engineering, Aarhus University, Aarhus C, 8000, Denmark.

https://doi.org/10.1016/j.jobe.2022.104026
Received 10 November 2021; Received in revised form 22 December 2021; Accepted 8 January 2022
Available online 13 January 2022

consumption by 5.8% between 2014 and 2017 and even more strongly, the building sector where the consumption rose by 8.3% in the same period [3].

Thus, it seems only logical to increase the building sector's effort to decrease its energy consumption. As new buildings should be nearly zero-energy buildings from 2021 onwards [4], the renovation of the building stock, where yet about 75% are energy inefficient buildings, becomes an essential tool, as about 80% of today's buildings will still be used in 2050 [5]. Despite this importance, the retrofitting rate in the EU remains at a low 1% [5].

One past project which aimed to increase this low retrofitting rate, was "School of the Future" [6]. Schools should thereby function as renovation demonstration projects, where pupils would consequently initiate a knowledge and experience transfer to their families and thus the retrofitting rate would increase. Next to this role as lighthouse projects, schools are also of particular importance as their indoor environmental quality (IEQ) directly influences the pupil's performance [7–9]. At the same time, recent studies in Denmark [10,11] showed that about 60% of the surveyed classrooms exceed the threshold of 1000 ppm CO_2-concentration set by the Danish building standard BR18 [1] and that 15% of the classrooms exceeded 25 °C [11]. A fact also reflected by a survey among pupils in Denmark [11] where students rated their satisfaction with the air quality between 35 and 55 out of 100, and 35 to 48 out of 100 for the classroom temperature. This negative influence on the performance also leads to considerable socioeconomic consequences, as shown by Wargocki et al. [12], who calculated for Denmark that an improvement of the indoor air quality (IAQ) could, on average, increase the public finances by €37 million per year and the gross domestic product by €173 million per year.

Given these points, the need for school renovations is undeniable. Common renovations often include the ventilation system, external walls, roof and windows [13]. However, the replacement of windows and insulation of the external envelope, particularly the wall, is often accompanied by a disturbance in school life due to noise and debris.

The ventilation system, crucial for a sufficient IAQ, imposes particular difficulties for school building renovation in Denmark. The reason for this is that most of the ventilation systems currently implemented in school buildings fail to provide a sufficient airflow [14], also shown indirectly by the high CO_2-concentrations in classrooms [10,11]. Consequently, a major renovation or a replacement of the existing ventilation system is often required. However, the current Danish building regulation BR18 [1] demands that if the existing ventilation system is entirely replaced or major alterations are conducted, it must fulfil the requirements for a new building. Thus, for schools, either a balanced ventilation system with a heat recovery efficiency of at least 73% must be used or a system that fulfils the requirements on an equal level without increasing the primary energy (PE) demand.

For school buildings with already existing balanced ventilation, this does not impose particular difficulties, nonetheless, for school buildings with exhaust ventilation which is currently used by every fifth building [11], a lack of space for ducts can be a crucial factor and an obstacle [15,16]. Current options to overcome this problem are decentral ventilation concepts that require a sufficient ceiling height, take up floor space, and need high maintenance [14].

Inspired by the above-outlined importance of school renovations and the challenges to be overcome, a novel renovation concept for schools is presented in this work which uses an exhaust ventilation system combined with a double skin facade (DSF) and diffuse ceiling ventilation (DCV) (Integrated Solution - Double Skin Facade and Diffuse Ceiling Ventilation for School Renovation (I-DIFFER)). Furthermore, based on a case study classroom, different configurations of I-DIFFER with varying glazing properties (number of panes, and physical properties) and DSF cavity thicknesses are compared against a range of traditional renovations by means of building performance simulation (BPS) using IDA-ICE 4.8 [17,18]. Thereby, it is evaluated if I-DIFFER can achieve a similar IEQ compared to a traditional renovation with an equal or lower total PE consumption. Additionally, the behaviour of I-DIFFER is analysed in detail for the summer and winter period. Finally, a sensitivity analysis is conducted for I-DIFFER, where the influence of the cavity thickness and glazing is investigated.

2. New system conceptualisation

Aiming to be a serious alternative to today's traditional renovation concepts, the fundamental design idea for I-DIFFER is to provide a less intrusive and more easily implementable solution. Thereby, two individual components, DSF and DCV play an essential role to facilitate this.

DSF, even though not universally defined, can be simplified seen as an external (outer) facade, an intermediate air space (cavity) and an inner facade. For I-DIFFER, the idea is to add a transparent outer layer to the existing facade of the building, which reduces the heating demand in the winter period [19] either in the occupied period, by preheating the supply air by utilising solar gains and partly recovering transmission losses [20] or in the non-occupied period, by creating a closed cavity which reduces transmission losses and increases the radiative temperature in the adjacent room. In contrast, a DSF can reduce the need for cooling during the summer [19]. For I-DIFFER, the cavity is ventilated with outside air, increasing transmission losses through the inner, unrenovated facade. Furthermore, as schools generally have high requirements for both fire and sound protection, the DSF is executed as one compartment per classroom, which prevents the spreading of fire, smoke and sound to adjacent rooms [21–23] and allows the use of a room wise control.

DCV, is an air distribution system where the whole or a large part of the ceiling is the supply opening. It consists of three central components: the room, the suspended ceiling panels and the plenum (a small room above the suspended ceiling). The air distribution pattern is controlled by buoyancy flows from heat sources [24] (up to 10 h^{-1} ACH [25]). In the recent past, the DCV driven by buoyancy gained more and more popularity in the non-industrial application as it can handle high loads and air flows without affecting the thermal comfort in terms of draught as the velocity is low [26–31]. Furthermore, several investigations already showed that cold air supply temperatures do not impose any draught issues [26,28,32,33]. Considering this, researchers found DCV a suitable system to be used in the context of classrooms as they concluded that it could not only improve the IAQ but also provides the necessary and sufficient thermal comfort [26,34–37] with the possibility to be implemented in already existing buildings without high investment cost [26,34,35].

Next to the DCV and the DSF, the **mechanical exhaust ventilation** ensures the necessary airflow in the classroom to maintain a good IAQ. In addition to these three components, a small bypass exists above the DSF, as shown in Fig. 1, to allow the intake of outside air without passing it through the DSF cavity avoiding preheating. To make use of these advantages, the new system can adapt to varying conditions where four airflow modes are known (Fig. 1):

- transparent insulation: all openings in cavity and bypass are closed - the ventilation is off.
- preheating mode: the ventilation is on - the air enters the DSF cavity at the bottom, leaves it at the top entering thereby the plenum and afterwards entering the room through the permeable ceiling.
- cooling mode: the ventilation is on - both external openings of the DSF cavity are open - air driven by wind and buoyancy ventilates the cavity. External and internal openings in the bypass are open - the air is driven by the ventilation enters the bypass, afterwards the plenum and through the permeable ceiling the room.
- cooling no ventilation mode: all external openings in the DSF cavity and the bypass are open - air driven by wind and buoyancy ventilates the large cavity and the bypass.

2.1. Sun shading

Additionally, I-DIFFER uses shading to reduce the risk of overheating, which is positioned on the inner side of the glazing of the DSF. This placement puts it as far outside as possible as this increases its efficiency [38,39] while still using the weather protection of the DSF. As a sun shading type, venetian blinds were deemed most suitable as their relatively large surface area allows for efficient extraction of heat if the cavity is ventilated [40]. For the radiative properties of the shading, the literature [22,39] is contradicting as to whether reflective or absorptive shading is more effective in reducing solar gains. However, a reflective shading independent of the effectiveness, was deemed more suitable as absorptive (dark) shading significantly reduced the illuminance in the adjacent room compared to a reflective (bright) one [39].

2.2. Openings

I-DIFFER has a total of five openings (Fig. 6 (a)) whereby only opening (2) and (3) are of importance for natural driven flow for DSF cavity. Thus these two openings are of particular importance as the opening area is correlated to the airflow rate for natural driven flow [41,42]. Additionally, it was decided to make the opening size of these openings in a ratio of 0.5:1, as the literature [39] indicated that this leads to lower cavity temperatures independent of the ratio direction, which is favourable for I-DIFFER as the cavity is only naturally ventilated for mode cooling (no vent.) (Fig. 3). The flow through the other opening (1), (4), and (5) is always mechanical driven and thus the size of these openings is not as critical as long as it is sufficient to not introduce a significant pressure drop.

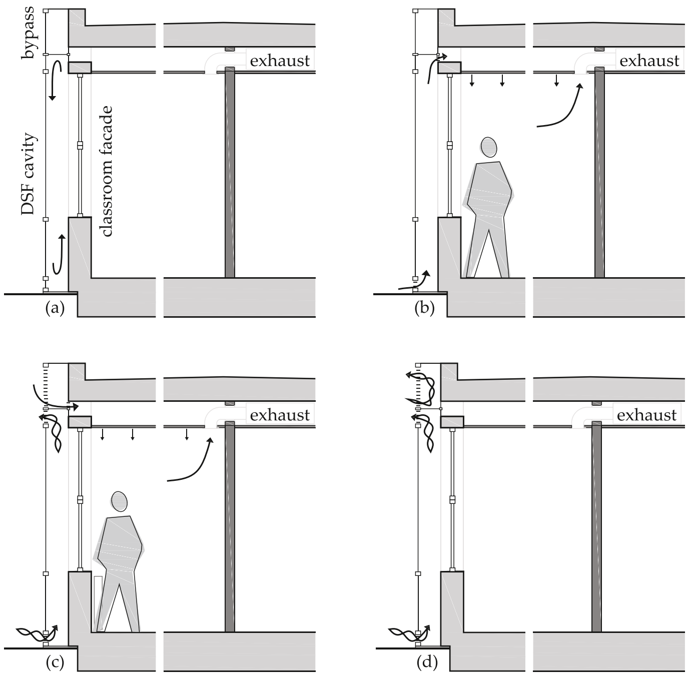

Fig. 1. Concept drawing of I-DIFFER showing its different operation modes: (a) transparent insulation, (b) preheating (c) cooling (d) cooling no ventilation. Arrows indicate the airflow paths.

2.3. Control

With the overall concept and its components defined, the next step was to define a control concept for the airflow modes (Fig. 2). In addition to the occupancy and the operative temperature of the classroom, the thermal neutral temperature of the occupants based on EN 16 798-1:2019-05 [43] were used. Furthermore, controllers with hysteresis were used to prevent cycling around the set point. The range of acceptable interior temperature varies between summer ($ORM_{30} \geq 10$ °C (ORM_{30} is the outdoor running mean temperature over the last 30 days excluding the current day)) and winter ($ORM_{30} < 10$ °C). As for winter, the PPD/PMV (cat. II) based approach is used, while for summer, the adaptive comfort model (cat. II) is applicable. The hysteresis was also adapted. For winter, the hysteresis was chosen as 2.5 °C, which leads to upper and lower limits of ±1.25 °C around the thermal neutral temperature. For summer, the hysteresis was set to 4 °C (±2 °C) and as the comfort boundaries are not symmetrical [43], the thermal neutral temperature was lowered by 0.5 °C to create symmetric limits. For both seasons, the offset from the hysteresis margins to the upper and lower limit of cat. II according to EN 16 798-1:2019-05 [43] were chosen to allow for expected under- and oversteering. An overview of all possible modes is given in Fig. 3.

The shading control is based on the one established by Karlsen et al. [44]. The IDA-ICE version used in this work does not allow the calculation of vertical eye illuminance. Therefore, the glare control is not implemented in the models. The cut-off angle was calculated as stated in Karlsen et al. [44], and the maximum of the cut-off angle and 15° was used. Furthermore, the control was adjusted based on the airflow pattern control (Fig. 2). Accordingly, the sun shading is never activated in the preheating mode but only during the cooling mode and during cooling no ventilation mode for solar gain control. Finally, the shading is activated in the transparent insulation mode if there is only little solar radiation to decrease heat losses. An overview of the resulting control is given in Fig. 3.

3. Case study

3.1. Typical classroom

To demonstrate the potential to achieve a good IEQ and to reduce the energy consumption of I-DIFFER, a representative case study for the Danish school building stock was defined and is consequently used for the BPS. Based on initial research [11,13,45] the case study object was defined as a south-facing classroom with an attached hallway in the north (Fig. 4). The room is located in Aalborg and in semi-exposed one-storey school building from the 1960s. The building is equipped with an exhaust ventilation system. Further characteristics, including occupancy and equipment, are shown in Table 1.

3.2. Assessment criteria

BR18 [1] requires that if school buildings do not use a balanced ventilation system with a heat recovery efficiency of 73%, it must be proven that the other system does not use more PE while providing the same conditions. However, as I-DIFFER affects more than just the ventilation system, this idea of a reference-based validation is extended to the whole classroom. Therefore, by comparing the PE consumption of the whole classroom for heating, ventilation, and lighting for I-DIFFER against one that was traditionally renovated, the overall performance of I-DIFFER can be assessed. The primary-energy factors used for electricity and for district heating were 1.9 and 0.85 [1].

Thermal comfort and IAQ are evaluated according to 'method A' as stated in CEN/TR 16 798-2:2019-05 [53]. For this method, the working hours within and outside the set limits are counted and the aim was set to be at least 94% of all working hours (2088 h) within the set limits. The limits of the cooling season follow the adaptive comfort model, whereas EN ISO 7730:2006-11 is used for the heating season. It is to be noted that as clothing is variable (Table 1) the limits for the winter period are not constant. A summary of the used criteria and their thresholds are given in Table 2.

3.3. Renovation

In the following, the two renovations scenarios are outlined. One scenario represents the traditional renovation, whereas the

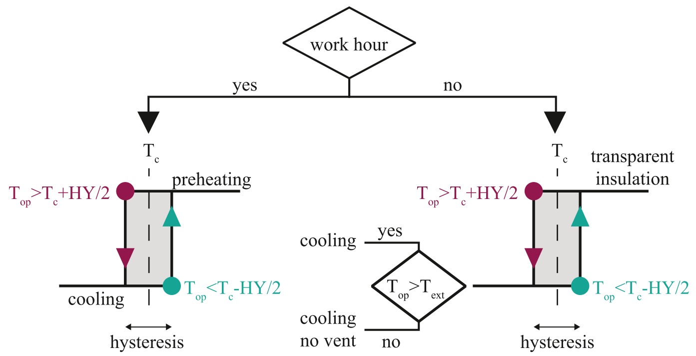

Fig. 2. Outline of airflow-pattern control for I-DIFFER. Cooling, preheating, transparent insulation and cooling no vent. refers to the operation modes of I-DIFFER (Fig. 1). HY = hysteresis (summer: 4 °C; winter: 2.5 °C); T_{ext} = external air temperature; T_c = thermal neutral temperature dependent on season (summer: $T_c = T_c$-0.5 °C; winter: $T_c = T_c$), T_{op} = classroom operative temperature.

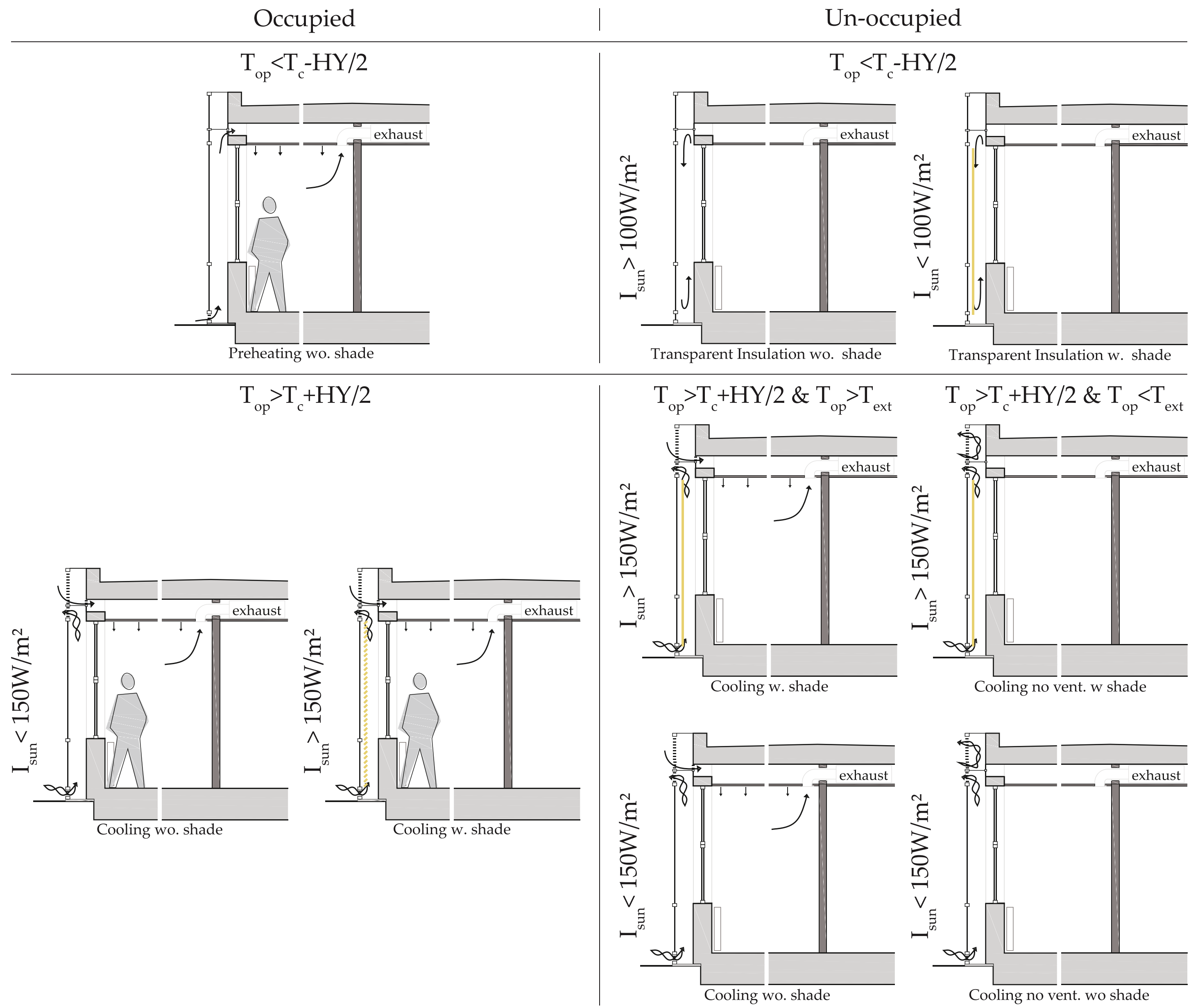

Fig. 3. Possible modes of I-DIFFER; yellow lines indicate venetian blinds; HY = hysteresis (summer: 4 °C; winter: 2.5 °C); T_{ext} = external air temperature; T_c = thermal neutral temperature dependent on season (summer: $T_c = T_c$-0.5 °C; winter: $T_c = T_c$), T_{op} = classroom operative temperature; I_{sun} = solar irradiation on facade. (For interpretation of the references to colour in this figure legend, the reader is referred to the Web version of this article.)

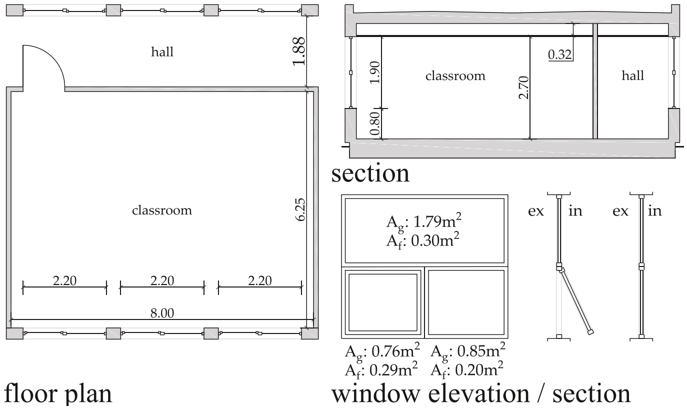

Fig. 4. Case study building: floor plan, section and window detail.

Table 1
Building and room characteristics for unrenovated school building; dimensions loosely based on [11,13,45]; properties without reference were defined by the authors.

characteristic	property	source
windows for classroom and hall		
parapet height	0.80 m	
glazing (two panes)	$U_g = 2.7$ W/(m^{2}K); g = 0.74; $\tau = 0.80$	[46]
frame	$U_f = 1.9$ W/(m^{2}K)	[46]
construction		
facade infill 62%	aerated concrete/insulation/brick - U = 0.50 W/(m^{2}K)	[47]
facade column 38%	aerated concrete/brick - U = 0.92 W/(m^{2}K)	[47]
floor	screed/concrete/expanded clay - U = 0.43 W/(m^{2}K)	[47]
roof	concrete/insulation - U = 0.45 W/(m^{2}K)	[47]
internal partition	gypsum/insulation	
internal ceiling	gypsum	
occupants		
nr.	20 students +1 teacher	[48]
activity level	1.2 met	
resting met. rate/srf. area	58.15 W/m^2 & 1.73 m^2	[49]
clothing	correlation on ORM_4 [a]	[50]
schedule	constant between 8:00-16:00	
equipment		
type	PC, projector, whiteboard, tablet	[51]
power total	757 W (15.14 W/m^2)	[52]

[a] 4-day outdoor running mean including the current day.

Table 2
Requirements and assessment criteria for traditional renovation and renovation with I-DIFFER.

criteria	threshold/unit	evaluation criterion		source
		I-DIFFER	Traditional	
requirements				
U-value wall	0.18 W/m [b]	–	✓	[1]
U-value roof	0.12 W/m [b]	✓	✓	[1]
E_{ref}	0.0 kWh	–	✓	[1]
artificial light	300 lx	✓	✓	[54]
assessment criteria				
PE cons.	kWh	$\leq PE_{trad}$ [a]	–	
thermal comfort	in Cat. II or I	94% of occ. time		[43] [b]
CO_2-conc.	<1000 ppm	94% of occ. time		[1]

[a] The traditional renovation sets the threshold.
[b] Humidity: 50%, velocity: 0.15 m/s.

second scenario describes an integration of the I-DIFFER system. The performance of the I-DIFFER solution in this work is evaluated in relation to the traditional renovation. Therefore, both scenarios are represented as design ranges and not as fixed design solutions. By identifying ranges, the performance of I-DIFFER can be better classified, but most importantly, it becomes independent of one specific traditional renovation. Looking upon I-DIFFER, the design ranges are established to gather knowledge about different configurations' performance and facilitate a sensitivity analysis.

3.3.1. Traditional renovation

Construction: The exterior wall of the classroom is insulated to achieve the area-averaged U-values shown in Table 3. The roof and exterior wall of the hallway, which only functions as a boundary, are renovated to the minimum BR18 requirements of 0.12 W/(m^2K) and 0.18 W/(m^2K) respectively. Infiltration is assumed to be 3.6 m^3/(h m^2) at a pressure difference of 50 Pa. Internal constructions and floor remain unchanged.

The window appearance remains unchanged (Fig. 4). The properties of the classroom window were changed according to Table 4. For double-glazing, the existing wooden frame remains (U_f = 1.9 W/(m^2K)), whereas for triple glazing a new frame (U_f = 1.0 W/(m^2K)) is chosen. The classroom window appearance and function remains unchanged (Fig. 4). The hallway windows' glazing was fixed to Double A1 (D-A1) (Table 4), with a respective U_f of 1.9 W/(m^2K).

Shading: As a shading system for the classroom, an external venetian blind is used. The control logic used is the same as for I-DIFFER and is based on Karlsen et al. [44], without glare control.

Technical system: A demand-controlled balanced ventilation based on CO_2-concentration and temperature is used. The system has a heat recovery efficiency of 73%, and the SFP is set to 1.8 kW/(m^3s). A heating coil supplied by district heating is installed in the ventilation unit, but no mechanical cooling exists. The desired supply temperature is set to 16 °C throughout the year during occupancy. Only the classroom is ventilated. The maximum airflow during operation was set to 18 m^3/(h m^2) (ACH = 6.67), while the minimum was set to 1.26 m^3/(h m^2), according to EN 16 798-1:2019 [43]. In winter, the system is turned off when occupancy ends and turned on 2 h before occupancy to provide the EN 16 798-1:2019 [43] demanded one ACH. In summer, the system can also run during unoccupied hours from Monday to Friday to provide night ventilation.

As heating, hydronic radiators were assumed with district heating as a carrier. The heating system is turned off when the ORM_{30} is above 10 °C the first time and turned on again when the ORM_{30} falls below 10 °C the first time.

The heating and cooling set-point of the classroom were set to the respective upper and lower comfort limits according to Subsection 3.2 with an offset of 0.25 °C. For the hallway, a constant heating set-point of 20 °C was used.

Lighting: Lighting is assumed to be replaced with efficient LED (max power: 3.4 W/m^2) controlled by presence and daylight. The daylight control is set according to the requirements. As efficiency 120 lm/W was set based on the average for developed countries [59].

3.3.2. Renovation with I-DIFFER

For I-DIFFER, the control as shown in Fig. 3 was used.

Construction: The exterior wall of the classroom is not altered. Only one additional facade layer is added to create the DSF (see *Transparent construction*). The roof and hallway wall are renovated as for the traditional renovation (Subsection 3.3.1). The current suspended ceiling is replaced with air-permeable wood-wool cement panels (thickness = 0.035 m), which provide a large opening area that is favourable if radiators are used for heating [26].

DSF - Transparent construction, cavity depth and openings: The glazing of the inner skin, i.e. the classroom windows, remains as defined in Table 1, assuming the windows are not replaced, the glazing and frame of the DSF are varied according to Table 5. The windows in the classroom can not be opened for the renovation with I-DIFFER.

As there is not one ideal cavity depth for the DSF, as this is a case-specific parameter which represents a trade-off between heating and cooling as they favour opposite trends [41,42] and is further influenced by the presence and properties of shading in the cavity [39] which is dynamic in the case of I-DIFFER, a range of depths (0.32 m, 0.43 m, 0.65 m, 0.81 m and 1.08 m) is analysed in this work.

Opening (2) and (3) (Fig. 6) were assumed to be multi-leaf dampers and set to be 0.15 m and 0.3 m high, respectively. They were assumed to be insulated in the case where double-glazing is used in the DSF with a U-value of 1.1 W/(m^2K) and to be not insulated if single-glazing is used. Opening (4) and (5) (Fig. 6 (a)) were assumed to be dampers each 0.1 m high.

Technical system: For I-DIFFER, the existing ventilation system is upgraded to be controlled by temperature and CO_2 controlled and to be sufficiently sized for today's demands (Section 1). The SFP, minimum and maximum ventilation flow is set as for the traditional renovation. If the ventilation system is activated outside the occupancy (I-DIFFER in cooling mode), it always runs at full capacity. The heating and cooling set-points are the same as for the traditional renovation.

Lighting: The lighting was set equal to the traditional renovation.

3.4. BPS model

Based on the renovation specifications (Section 3.3) the IDA-ICE model for the traditional renovation and I-DIFFER are outlined. First, the common characteristics are presented before the individual approaches for each case are discussed. Additional supplementary information regarding the model used can be found in Appendix A.

For both renovations, the Danish design reference year (2010) version 3 [60] was used. The outside air CO_2-concentration was set to 400 ppm. The suspended ceiling in the hallway and classroom were modelled as separate thermal zones, so was the DSF for I-DIFFER

Table 3
Area averaged U-value for the classroom exterior wall, assuming a λ = 0.035 W/(m K) for the new and λ = 0.050 W/(m K) for the old insulation.

		variations	
U-value wall [W/(m^2K)]	0.18	0.14	0.10

Table 4
Traditional renovation glazing, E_{ref} calculated according to BR18 [1]. All glazing properties but for Tripe A1 taken from Ref. [55]; Triple A1 properties taken from Ref. [56]. U_g based on EN 673:2011-02 [57]; g and τ based on EN 410:2011-02 [58].

name	U_g [W/(m^{2}K)]	g	τ	E_{ref} [kWh/(m^{2}a)]
double-glazing - U_f = 1.9 W/(m^{2}K)				
Double A1 (D-A1)	0.9	0.52	0.71	1.83
Double B1 (D-B1)	1.0	0.62	0.82	14.33
Double B2 (D-B2)	1.2	0.62	0.82	0.05
Double C1 (D-C1)	1.1	0.71	0.83	24.87
Double C2 (D-C2)	1.4	0.71	0.83	3.45
triple glazing - U_f = 1.0 W/(m^{2}K)				
Triple A1 (T-A1)	0.5	0.33	0.61	10.14
Triple B1 (T-B1)	0.5	0.47	0.70	37.64
Triple B2 (T-B2)	0.7	0.47	0.70	23.36
Triple C1 (T-C1)	0.5	0.60	0.77	63.17
Triple C2 (T-C2)	0.7	0.60	0.77	48.90

Table 5
I-DIFFER DSF glazing. Glazing properties taken from Ref. [55]. U_g based on EN 673:2011-02 [57]; g and τ based on EN 410:2011-02 [58].

	U_g [W/(m^{2}K)]	g	τ
single-glazing - U_f = 5.0 W/(m^{2}K)			
Single A1 (S-A1)	5.8	0.88	0.91
Single B1 (S–B1)	5.7	0.70	0.67
Single C1 (S–C1)	5.8	0.57	0.51
Single D1 (S-D1)	5.8	0.44	0.37
double-glazing - U_f = 1.5 W/(m^{2}K)			
Double B1 (D-B1)	1.0	0.62	0.82
Double B2 (D-B2)	1.2	0.62	0.82
Double C1 (D-C1)	1.1	0.71	0.83
Double C2 (D-C2)	1.4	0.71	0.83
Double D1 (D-D1)	2.7	0.80	0.83
Double E1 (D-E1)	1.0	0.33	0.70

(Fig. 5). Internal loads were defined according to Table 1. The infiltration was distributed to the thermal zone according to their external surface area.

Windows were modelled using the pane-by-pane model (`DetWind`). The radiators were simplified to generic room units without a given physical location, whose share of longwave radiation was set to 0.4, which is area-proportional distributed to all room surfaces. An illustration of the simulation model is shown in Fig. 5.

3.4.1. Traditional renovation model

For the classroom, the opening of the openable part was set to 90% of its width and 36% of its height. The ventilation system was modelled using the "Standard air handling unit" with the supply and exhaust in the classroom zone. The power of the heating coil in the ventilation unit was set to infinite large and its efficiency to 1.0.

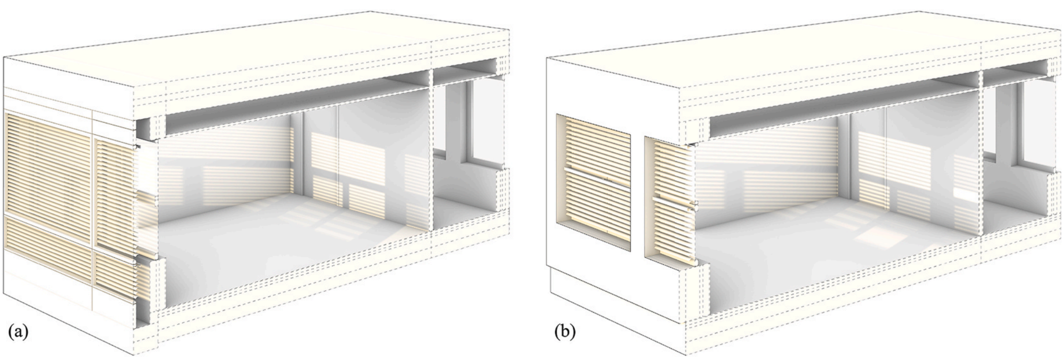

Fig. 5. Illustration of the simulation model as a 3D section; (a) I-DIFFER (b) traditional renovation.

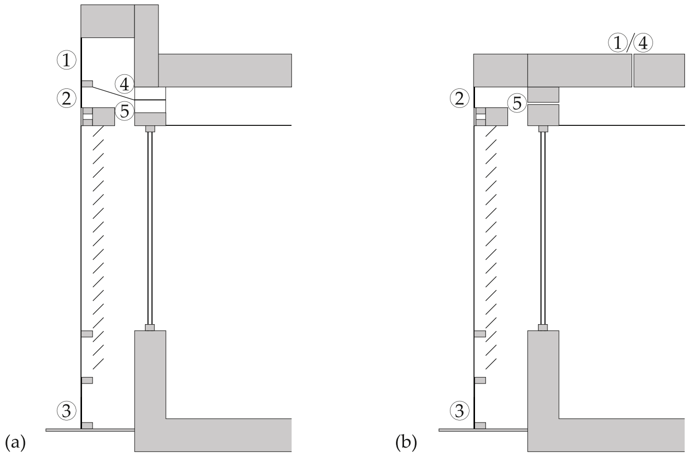

Fig. 6. Simplification of openings (current mode: transparent insulation) from (a) actual situation to (b) simplified simulation model. Numbers are used to indicate different openings. Illustration only.

3.4.2. I-DIFFER renovation model

Opening (2) and (3) were modelled as windows with a frame ratio of just below one (one is not possible) to represent opaque openings. The construction was defined as two aluminium sheets with insulation with a U-value of 1.1 W/(m^2K) for the double-glazing and only 3 mm aluminium without insulation for single-glazing. The openable area was set to 97% and 81% of their width and height. The C_d value was set to 0.65. To avoid bidirectional flow in preheating mode (Fig. 3), opening (3) is opened only at 10% while it is opened at 100% in cooling mode to generate the highest flow possible.

Opening (5) (Fig. 6) was represented using a leak (given flow) component. This was done as a leak component reduces the model complexity compared to a large vertical opening component and as the volume flow through opening (5) is determined by the ventilation system and is therefore known. The leak was controlled accordingly.

Another simplification was necessary due to the geometry of the case study. Due to the low suspended ceiling height of only 0.32 m, the separation between upper and lower DSF cavity could not be straight (Fig. 6) (a) as otherwise, the case of the shading would be in front of the classroom's window. However, only rectangular zones can be modelled with the detailed zone model in IDA-ICE, the approach used is shown in Fig. 6 (b). The upper zone (bypass) was not modelled and opening (1) and (4) was replaced by a leak (given flow) component in the roof. This approach seems at first sight as an extreme alteration from the original design, but one needs to keep in mind that each zone in IDA-ICE assumes perfect mixing and thus the location of the leak is not essential for the zone. Furthermore, the airflow through opening (4) is only controlled by mechanical ventilation and is therefore also known. Moreover, the expected temperature increases from the supply via opening (1) and (4) through the bypass is slight, so that a direct supply of outdoor air seems reasonable.

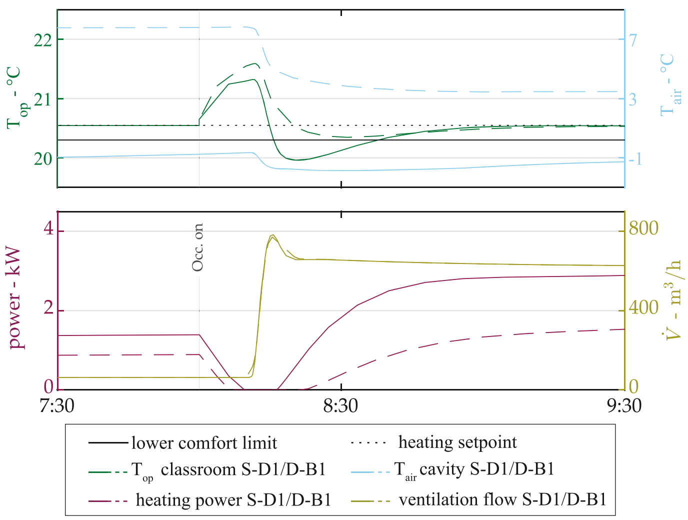

Fig. 7. Detailed analysis of hours below the comfort limit of I-DIFFER on the 20th of December. Model with highest (glazing S-D1 (Table 5) cavity thickness = 1.08 m) and lowest (glazing D-B1 (Table 5) cavity thickness = 0.32 m) numbers of occupied hours below the comfort limit.

The diffuse ceiling panels were also modelled as a leak (pressure-dependent flow) with an equivalent leakage area of 1.07 m^2 at 4 Pa calculated based on the flow rate obtained from Ref. [25] for wood-wool cement panel assuming an air density of 1.21 kg/m^3. The exhaust ventilation system was modelled as a "VAV-exhaust ventilation system" with the exhaust located in the classroom.

4. Results

4.1. Thermal comfort and IAQ

All variations of the traditional renovation and the renovation with the novel system were within the desired range for the CO_2-concentration (<1000 ppm, Table 2) for at least 99% of the occupied time. This confirms that the ventilation airflow rate is sufficient and the control works as intended.

For the global thermal comfort of the traditional renovation, 8 out of 30 simulations were invalid as they were inside the thermal comfort limits (Table 2) less than 94% of the occupied time, whereby all simulation almost exclusively showed the trend to be above the comfort limits but not to be below. The invalid simulations are thereby exclusively combinations with double-glazing D-B1, D-B2, D-C1 and D-C2, thus glazing with high g-values, whereby the trend was seen that a low U-value of the exterior wall was beneficial to stay within the thermal comfort limits.

For the renovation with I-DIFFER, 40 of the conducted 50 simulations were within the comfort limits at exactly or above 94% of the occupied time. The hours outside this range were mainly too warm, but hours below the comfort range also existed. Further analyses were conducted to identify when underheating occurs and the reason such a large share of underheating (up to 1.3% of occupied time) exists, despite a sufficient sized heating system. This revealed that underheating occurs in winter when single-glazing in the external layer of DSF is used. Fig. 7, where I-DIFFER is in preheating mode, compares the best (D-B1, Table 5 and cavity thickness = 1.08 m) and the worst model (S-D1, Table 5 and cavity thickness = 0.32 m) in terms of underheating. The interaction of increasing ventilation flow, cold supply temperature (cavity temperature), and sudden increase of internal heat gains, due to the start of occupancy and the delay of the PI controller used for the heating control, results in underheating of the occupied space, which is characteristic for the morning hours when the occupancy begins. The ventilation rate thereby increases after the start of the occupancy as the ventilation flow is controlled by the CO_2-concentration in the classroom.

4.2. Primary energy

In the next step, the PE consumption for indoor comfort valid simulations of the traditional renovation (number of simulations: n = 22 out of 30) and renovation with I-DIFFER (n = 40/50) were compared against each other. First the individual shares, heating,

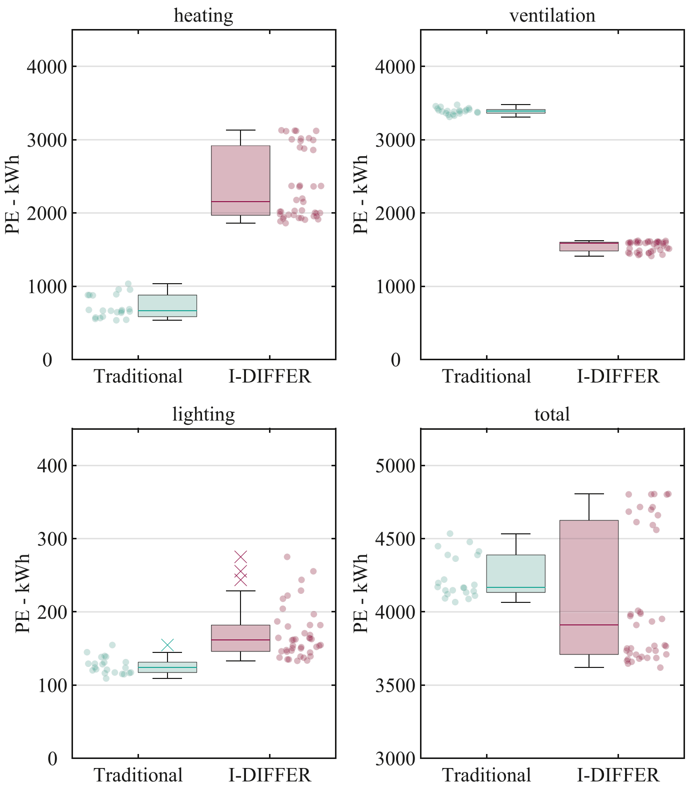

Fig. 8. PE for heating, ventilation and lighting, and total PE. Heating of the traditional renovation contains both the space heating of the classroom as well as the heating coil of the ventilation. Circles belong to sample data points. Traditional n = 22/30; I-DIFFER n = 40/50.

ventilation, and lighting were analysed before the total PE consumption were compared.

For the PE for heating (Fig. 8), the consumption of I-DIFFER can be more than three times higher compared to the lowest result of the traditional renovation. However, a clear separation in two groups is visible for I-DIFFER, whereby the upper group consists solely of single-glazing and the lower group of double-glazing. An overall opposite trend to heating is visible for the PE for ventilation (Fig. 8), where I-DIFFER consumes less than half compared to the traditional renovation. A reduction of about half can be explained by the difference in the ventilation systems of the traditional renovation and I-DIFFER. While the greater reduction is caused by the fact that the average ventilation volume flow in summer is for I-DIFFER about 19% lower than for the traditional renovation, the winter difference is negligible. The reason for this reduction in summer could be that shading is more effective for I-DIFFER, that the unrenovated classroom facade of I-DIFFER allows for higher heat losses if desired or the different control strategy of the two systems. Focusing now on PE of lighting (Fig. 8), I-DIFFER shows overall a higher consumption, which can relate to the total lower visible transmittance of I-DIFFER (outer and inner glazing combined). Moving on to the total PE consumption (Fig. 8), which is the sum of the PE for heating, ventilation and lighting, I-DIFFER shows overall a larger variation than the traditional renovation. Therefore, two distinct groups are visible, whereby the lower consists only of configurations with double-glazing while the upper one only includes configurations with single-glazing. The upper group leads exclusively to a PE consumption higher than the worst traditional renovation while all configurations of the lower group outperform the best traditional renovation. As result from the 40 I-DIFFER configurations that had a valid user comfort, 28 have a total PE consumption equal or smaller to the total PE of the worst traditional renovation and are thus valid for energy. From this analysis, it can be concluded that the PE for heating is the main determining factor for the PE consumption of I-DIFFER while the PE for ventilation is more important for the traditional renovation. Additionally it can already be said that the difference between single and double-glazing in the outer layer of the DSF is significant and that single-glazing leads to a worse performance than the worst traditional renovation.

4.3. Detailed system analysis

To obtain more insight into how I-DIFFER behaves in detail, two three-day periods in summer and winter were analysed for I-DIFFER. To avoid distortion of the result, only simulations valid for both energy and indoor comfort are considered (n = 28/50). It should be noted that shading and mode in Figs. 9 and 10 represent all shown solutions above each other, i.e. in this case, where n = 28,

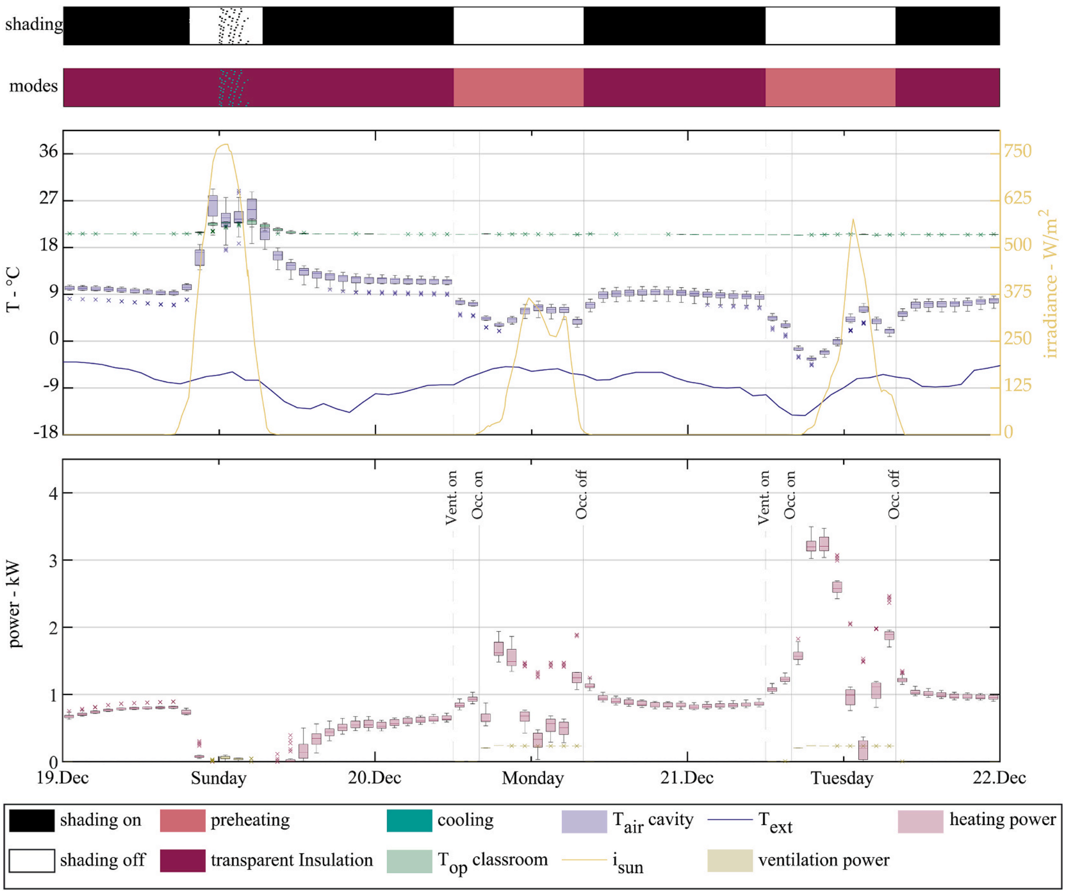

Fig. 9. I-DIFFER's performance for an exemplary three-day winter period. i_{sun} = solar irradiation on facade; hourly averages of heating power, ventilation power, T_{air} cavity, T_{op} classroom; instantaneous values for modes, shading, i_{sun} and T_{ext}. Modes and shading represent all variations as lines above each other. I-DIFFER n = 28/50.

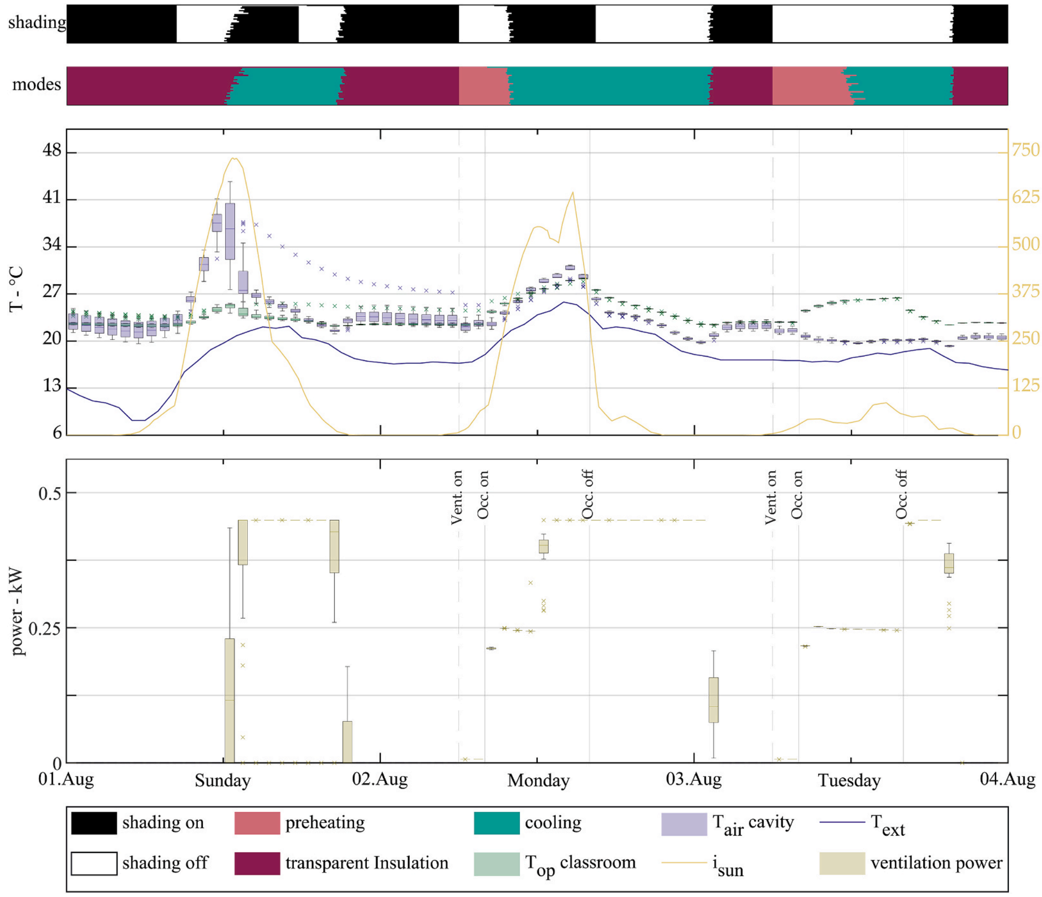

Fig. 10. I-DIFFER's performance for an exemplary three-day summer period. i_{sun} = solar irradiation on facade; hourly averages of heating power, ventilation power, T_{air} cavity, T_{op} classroom; instantaneous values for modes, shading, i_{sun} and T_{ext}. Modes and shading represent all variations as lines above each other. I-DIFFER n = 28/50.

there are 28 lines above each other. All box plots represent hourly mean values of the respective quantity. The wind velocity and direction are not shown as no influence could be seen. This indicates that the airflow in situations where the DSF cavity is naturally ventilated is mainly buoyancy driven.

4.3.1. Winter period

The results for winter (Fig. 9) show the expected strong influence of the solar irradiation on the facade for the transparent insulation mode, while the outdoor temperature is determining for the preheating mode. The strong influence of solar irradiation on the heating also leads to fast-changing loads, where within 3 h, the load can vary by about 3.5 kW as seen on the 21st December (Fig. 9). From this, it can also be concluded that high peak loads can occur on each occupied day if the outdoor temperature and solar irradiation are low. Furthermore, in occupied periods with solar irradiation, the negative influence of glazing with a low g-value, indicated by the upper outlier of the heating power, can be seen. In addition, it can be noted that no heating is required on days with no occupancy if the solar irradiation is high. In this situation, the cavity temperature also rises to 36 °C above the outdoor temperature. At the conditions of low ambient temperature and high solar irradiation, rapid cycling between transparent insulation mode and cooling mode occur as the high volume flow and the activated shading in cooling mode leads to a rapid decrease of the operative classroom temperature. At the same time, it consequently rises fast in transparent insulation mode.

4.3.2. Summer period

The summer period (Fig. 10) again shows a strong influence of both solar irradiation as well as ambient temperature. Furthermore, it can be seen that preheating is frequently used in summer at the beginning of a day but also till around midday if solar irradiation is low. The effectiveness of the cooling mode to reduce the cavity temperature to be close to the outdoor temperature is shown for both Sunday and Monday (1st and 2nd August), where, despite high solar irradiation on the facade, the cavity temperature does not rise more than 7 °C above the outdoor temperature. Additionally, it can be seen that on Sunday, one model (cavity thickness of 1.08 m and glazing D-E1) does not switch into cooling mode and has a significant higher cavity and classroom temperature (upper outlier) than the others. Consequently, this model also switches into cooling mode first on the following Monday due to its higher temperatures.

4.4. Sensitivity analysis

From the above-shown results, it is shown that I-DIFFER has the potential to perform significantly better for the PE consumption compared to the traditional renovation but can also perform worse. So far it is only known that single- and double-glazing leads to a clear difference in the PE consumption (Subsection 4.2), but apart from that, the influence of glazing properties and cavity thickness is unknown. Following a visual sensitivity analysis, employing scatter plots, is conducted to obtain knowledge about how the three altered parameters influence the PE consumption and the user comfort of the new system.

Beginning with the total PE consumption (Fig. 11), it can be seen that the different glazing causes the most substantial variation with a clear difference between single and double-glazing. For the double-glazing, a positive trend towards glazing D-B1, D-B2, D-C1 and D-C2 is visible, thus favouring low U-values with high g-values. This is confirmed by glazing D-E1 ($g = 0.33$), which, even though it has the same U-value as D-B1, performs worse. It is to be noted that D-D1 and D-E1 lead to total PE consumption in the same range even though they have contrary properties (high U-value and g-value and low U-value and g-value). This shows the direct interaction between U-value and g-value. For the thickness of the DSF cavity, the differences between variations are barely noticeable. For the numerical values, it can be seen that the total PE decreases with increasing cavity thickness.

The same pattern as described for the total PE consumption can also be seen for the PE for heating (Fig. 11). The similarity between total PE and PE for heating highlights again that heating is due to its high magnitude and significant variation, the determining factor for the total PE consumption of I-DIFFER.

A contrary trend to the above shows the PE for ventilation (Fig. 11). While the glazing still has the greatest influence overall, the opposite trend as before can be seen. All double-glazing apart from D-E1 show worse results compared to the single-glazing S–B1 to S-D1, whereby the single-glazing shows a trend favouring low g-values. This trend also explains why glazing S-A1 is the worst single-glazing as it has the highest g-value compared to all other glazing. The similar result of D-E1 and S-D1 show that the U-value is of minor importance compared to the g-value. This is also conclusive given that the ventilation varies in a minor way in winter between the simulations but more significantly in summer. Additionally, a minor influence of the DSF cavity thickness is visible, showing a decreasing PE consumption for increasing thickness.

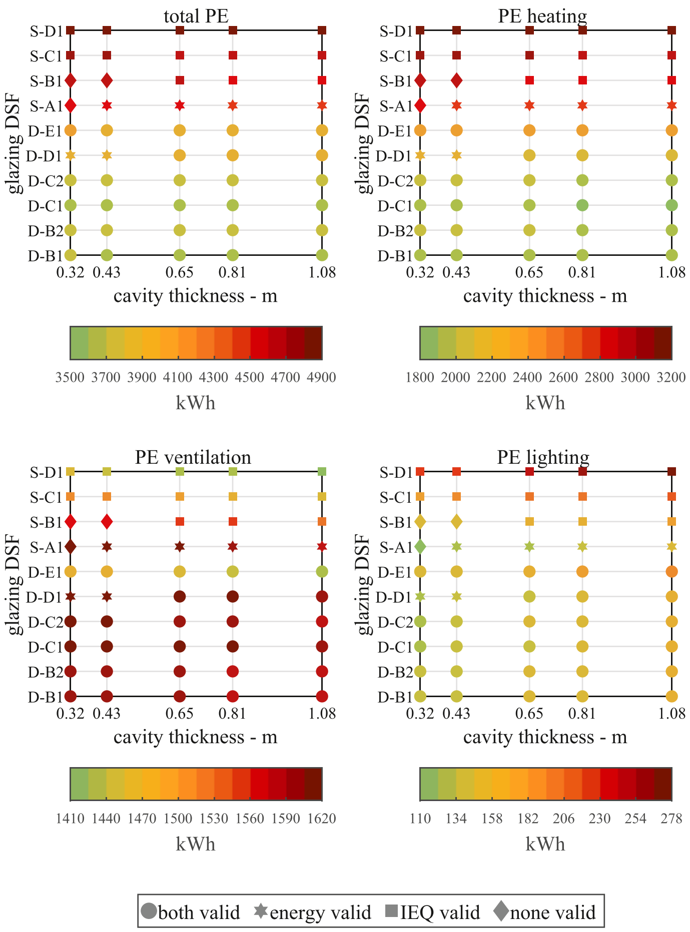

Fig. 11. Total PE, heating, ventilation and lighting PE. I-DIFFER n = 50/50.

The same pattern as the PE of ventilation shows the hours above the comfort limit (not shown), indicating the close relation of ventilation and overheating.

The PE for lighting (Fig. 11) follows, as expected, the trend of the visible transmittance for the glazing. For the cavity thickness, the PE increases with increasing thickness.

Focusing on the valid simulations (Fig. 11), it can be seen that all double-glazing (apart from D-D1) in combination with the two narrowest cavities are valid for both energy and user comfort. However, the user comfort causes the invalidity of the D-D1 configurations. As mentioned before, all single-glazing is invalid, whereby S–C1, S-D1 (low g-values) and S–B1 for large cavity thicknesses are valid for user comfort but have a higher PE consumption than the traditional renovation. In contrast, glazing S-A1 for all but the narrowest cavity is valid for energy but not user comfort.

The overall best result in terms of total PE consumption and valid user comfort is the combination of the deepest cavity (1.08 m), together with double-glazing D-C1 ($U = 1.1$ W/(m^2K) $g = 0.71$).

5. Discussion and conclusion

With the aim to offer a serious alternative to traditional renovations, this work proposed a new, less intrusive renovation concept for schools - I-DIFFER - combining DCV with DSF and exhaust ventilation. First, a concept showing the operation modes, the system's components and the control strategy was presented. In addition, this concept was applied to a representative case study classroom. Furthermore, the potential I-DIFFER was illustrated through BPS where 50 I-DIFFER configurations with varying DSF cavity thickness and glazing were compared against 30 traditional renovation configurations with varying glazing and external wall insulation.

Compared to a traditional renovation where windows are replaced and the exterior wall is insulated, I-DIFFER could, for a south-facing classroom, achieve up to 11% lower PE consumption comparing the lowest PE of the traditional renovation to the lowest PE of I-DIFFER. Consequently, it can be said that I-DIFFER is a competitive approach to traditional renovation, which offers a new possibility to engineers and architects. Overall, 28 out of 50 I-DIFFER configurations satisfied the IEQ requirements used and consumed less PE than the worst traditional renovation that satisfied the IEQ. Thereby all of these configurations used double-glazing for the DSF. Furthermore, the results showed that the PE for heating has a superior influence compared to the PE for ventilation on the total PE for I-DIFFER, while the opposite was shown for the traditional renovation. Further studies revealed that for single-glazing (and to a lesser extent for double-glazing), underheating can occur at the beginning of occupancy in cold periods despite sufficient heating power. This is due to an interaction of the heating control cold supply temperature and increasing ventilation flow.

The conducted sensitivity analysis for I-DIFFER showed that the glazing has a superior influence compared to the cavity thickness. Thereby the analysis showed that for heating, a low U-value and high g-value leads to the lowest demand, while for ventilation, the opposite was shown. Ventilation PE showed a more negligible influence by the varied factors compared to heating. Even though the cavity thickness had a small influence overall, it could be seen that for the total PE consumption, the deepest cavity thickness achieved the lowest PE whereby heating and ventilation PE, as part of the total PE, both decreased with increasing cavity thickness.

Detailed analysis of three-day periods in summer and winter showed that the airflow modes and shading work as intended. The analysis showed that the ambient temperature and the availability of solar irradiation on the facade significantly influence the system's performance. For the winter period, it was also seen that due to the critical influence of solar irradiation, the heating power could shift by about 3.5 kW within 3 h, highlighting that a fast-reacting heating system is necessary. Furthermore, it was seen that fast cycling of modes occurs during non-occupied periods in winter with high solar irradiation on the facade and low ambient air temperatures. To avoid such cycling, the shading control could be adjusted to stay permanently closed during non-occupied periods. However, in winter this could lead to an increase in heating energy during the day.

While this work demonstrates the overall potential of I-DIFFER for Denmark, its application is not limited to Denmark alone and future work should investigate this possibility for other countries' climates. Additionally, this work only investigated a south-oriented classroom. Therefore, the applicability of I-DIFFER for other orientations should be analysed in subsequent work where it is expected that the PE consumption of I-DIFFER increases due to reduced solar irradiation. While this work mainly focused on the thermal IEQ, questions regarding, e.g., the visual or acoustic IEQ remain uncertain and should be addressed by future research. Additionally, a life cycle analysis could allow for valuable knowledge about I-DIFFER's economic and environmental usefulness. Finally, I-DIFFER should also be studied through an experiment to validate the results of this work.

CRediT authorship contribution statement

Laura Bugenings: Conceptualisation, Methodology, Formal analysis, Writing - Original - Draft, Writing - Review & Editing, Visualisation.

Markus Schaffer: Conceptualisation, Methodology, Formal analysis, Writing - Original - Draft, Writing - Review & Editing, Visualisation.

Olena Kalyanova Larsen: Conceptualisation, Supervision, Funding acquisition, Writing- Review & Editing.

Chen Zhang: Conceptualisation, Supervision, Funding acquisition, Writing- Review & Editing.

Funding

This work has been supported by the Energy Technology Development and Demonstration Program (EUDP) under the name I-DIFFER (Journal number: 64 020–2140), Denmark.

Declaration of competing interest

The authors declare that they have no known competing financial interests or personal relationships that could have appeared to influence the work reported in this paper.

Appendix A. Simulation model specifications

In the following, more detailed specifications of the used BPS model for IDA- ICE are given. First, information valid for both renovation scenarios is presented. Next, the information only valid for the traditional renovation is shown.

To consider shading from the remaining building and to obtain more accurate ground temperatures, the building itself was modelled 40.625 m long assuming five classrooms next to each other, and the simulated one was placed in the middle.

All zones were modelled with the detailed zone model (CeDetZon) of IDA-ICE. For all zones, convective heat transfer coefficient algorithm 3 (Max(BRIS Model, CD Model)) was used. It should be noted that the selection of this specific algorithm imposes an uncertainty especially for the DSF and plenum zones as the heat transfer coefficient was shown to have a significant influence [61–67] and yet no overall accepted superior algorithm is known for these components. To account for the furniture in the classroom, 11 tables á 1.12 m^2 and 21 chairs á 0.16 m^2 were assumed.

The standard wall model (BDFWall) was used for external construction and constructions separating zones, whereas the adiabatic wall model (AdWall) was used for internal constructions. For the classroom, each window part was modelled with an individual window model (three window models per window), the hallway windows were simplified modelled as one window component per window (Fig. 5).

The motor of the fan of the ventilation system was set to be in the air and 100% of its energy contributes to the air temperature rise. Its performance under partial load was set to the default value in IDA-ICE (according to ASHREA Standard 90.1-2007 appendix G). The total fan system efficiency was set to 0.6.

Appendix A.1. Traditional renovation

To mimic the manual operation of the openable classroom window the openable parts were controlled by temperature and schedule. The windows were opened when the outside temperature was lower than the classroom operative temperature, the operative classroom temperature had surpassed the cooling setpoint minus 1.5 °C, the classroom was occupied and the ORM_{30} was higher than 10 °C. The minimum time between cycles of operation was set to 600 s.

References

[1] Trafik- Bygge og Boligstyrelsen, Bygnings reglementet 18, 2018. bygningsreglementet.dk.
[2] European Environment Agency, Trends and Projections in Europe 2020 - Tracking Progress towards Europe's Climate and Energy Targets, Tech. Rep. 13/2020, European Environment Agency, Copenhagen, 2020, https://doi.org/10.2800/830157, https://www.eea.europa.eu/ds_resolveuid/47fda3c1ea3049f096a99ec24c9ae98f.
[3] European Environment Agency, Trends and Projections in Europe 2019 - Tracking Progress towards Europe's Climate and Energy Targets, Tech. Rep. 15/2019, European Environment Agency, Copenhagen, 2019, https://doi.org/10.2800/51114.
[4] European Commission, Energy Performance of Buildings Directive, 2021. Retrieved: 2020-08-03, https://ec.europa.eu/energy/topics/energy-efficiency/energy-efficient-buildings/energy-performance-buildings-directive_en.
[5] European Commission, Renovation Wave, 2020. Retrieved: 2020-08-03, https://ec.europa.eu/energy/topics/energy-efficiency/energy-efficient-buildings/renovation-wave_en.
[6] H. Erhorn-Kluttig, S. Doster, H. Erhorn, Tech. Rep., School of the Future - Towards Zero Emission with High Performance Indoor Environment, 1, European Union, 2016 https://www.school-of-the-future.eu/images/files/20160310BrochureSchoolOfTheFutureUK.pdf.
[7] P. Wargocki, D.P. Wyon, The effects of outdoor air supply rate and supply air filter condition in classrooms on the performance of schoolwork by children (RP-1257), HVAC R Res. 13 (2) (2007) 165–191, https://doi.org/10.1080/10789669.2007.10390950. ISSN 1078-9669, http://www.tandfonline.com/doi/abs/10.1080/10789669.2007.10390950.
[8] P. Wargocki, D. Wyon, The effects of moderately raised classroom temperatures and classroom ventilation rate on the performance of schoolwork by children (RP-1257), HVAC R Res. 13 (2) (2007) 193–220, https://doi.org/10.1080/10789669.2007.10390951. ISSN 1078-9669, http://www.tandfonline.com/doi/abs/10.1080/10789669.2007.10390951.
[9] WHO Regional Office for Europe, School Environment: Policies and Current Status, Tech. Rep., World Health Organisation, Copenhagen, 2015.
[10] D.P. Wyon, P. Wargocki, J. Toftum, G. Clausen, Classroom ventilation must be improved for better health and learning, REHVA J. 47 (7) (2010) 35–39.
[11] DTU, Tech. Rep, Indeklima i skoler - WP 2.1: identifikation af karakteristika for skolebygninger med dårlig og god luftkvalitet ud fra let tilgængelige data om skolebygningerne, 1, Center for Indeklima og Energi ved Danmarks Tekniske Universitet, 2016.
[12] P. Wargocki, P. Foldbjerg, K.E. Eriksen, L.E. Videbæk, Socio-economic consequences of improved indoor air quality in Danish primary schools, in: 13th International Conference on Indoor Air Quality and Climate International Conference on Indoor Air Quality and Climate, International Society of Indoor Air Quality and Climate, 2014.
[13] DTU, Tech. Rep, Indeklima i skoler - WP 1.1: oversigt over skolerenoveringer med fokus på at skabe bedre indeklima,, 1, Center for Indeklima og Energi ved Danmarks Tekniske Universitet, 2016.
[14] C.A. Hviid, S. Petersen, Evaluation of ventilation solutions for retrofitting of schools, in: 36th AIVC Conference: Effective Ventilation in High Performance Buildings, 2015, pp. 959–967. Madrid.

[15] M. Mysen, P.G. Schild, V. Hellstrand, K. Thunshelle, Evaluation of simplified ventilation system with direct air supply through the facade in a school in a cold climate, Energy Build. 37 (2) (2005) 157–166, https://doi.org/10.1016/j.enbuild.2004.05.010. ISSN 3787788, https://linkinghub.elsevier.com/retrieve/pii/S0378778804001689.

[16] C.A. Hviid, S. Petersen, Implementation of ventilation in existing schools - a design criteria list towards passive schools, in: Proceedings of Passive House Symposium, 2012. Bruxelles.

[17] A.B. EQUA Simulation, IDA-ICE - IDA Indoor Climate and Energy, 2020. https://www.equa.se/en/.

[18] P. Sahlin, L. Eriksson, P. Grozman, H. Johnsson, A. Shapovalov, M. Vuolle, Whole-building simulation with symbolic DAE equations and general purpose solvers, Build. Environ. 39 (8) (2004) 949–958, https://doi.org/10.1016/j.buildenv.2004.01.019. ISSN 3601323, https://linkinghub.elsevier.com/retrieve/pii/S0360132304000307.

[19] F. Pomponi, P.A. Piroozfar, R. Southall, P. Ashton, E.R. Farr, Energy performance of Double-Skin Façades in temperate climates: a systematic review and meta-analysis, Renew. Sustain. Energy Rev. 54 (2016) 1525–1536, https://doi.org/10.1016/j.rser.2015.10.075. ISSN 13640321, https://linkinghub.elsevier.com/retrieve/pii/S1364032115011545.

[20] D. Saelens, J. Carmeliet, H. Hens, Energy performance assessment of multiple-skin facades, HVAC R Res. 9 (2) (2003) 167–185, https://doi.org/10.1080/10789669.2003.10391063. ISSN 1078-9669, http://www.tandfonline.com/doi/abs/10.1080/10789669.2003.10391063.

[21] E. Oesterle, R.-D. Lieb, M. Lutz, W. Heusler, Double-Skin Facades: Integrated Planning, 1 edn., Prestel Verlag, Munich, 2001. ISBN 3-7913-2504-3.

[22] D. Saelens, Energy Performance Assessment of Single Storey Multiple-Skin Facades, Ph.D. thesis, Catholic University of Leuven, 2002.

[23] T. Herzog, R. Krippner, W. Lang, Facade Construction Manual, 2 edn., Detail Business Information GmbH, München, 2017. ISBN 9783955533700.

[24] D. Müller, C. Kandzia, R. Kosonen, A.K. Melikov, P.V. Nielsen, Mixing Ventilation Distribution Design, Rehva Guidebook No. 19, REHVA, 2013. ISBN 9782930521114.

[25] C. Zhang, T. Yu, P.K. Heiselberg, M.Z. Pomianowski, P.V. Nielsen, Diffuse Ceiling Ventilation - Design Guide for Wood Wool Cement Panel, Tech. Rep., Department of Civil Engineering, Aalborg University, 2017.

[26] P. Jacobs, E.C.M.V. Oeffelen, B. Knoll, Diffuse ceiling ventilation, a new concept for healthy and productive classrooms, Indoor Air (2008) 17–22. August.

[27] P.V. Nielsen, E. Jakubowska, The performance of diffuse ceiling inlet and other room Air distribution systems, in: Cold Climate HVAC, Sisimiut Greenland, 2009.

[28] C.A. Hviid, S. Svendsen, Experimental study of perforated suspended ceilings as diffuse ventilation air inlets, Energy Build. 56 (2013) 160–168, https://doi.org/10.1016/j.enbuild.2012.09.010. ISSN 3787788, doi:10.1016/j.enbuild.2012.09.010.

[29] J. Fan, C.A. Hviid, H. Yang, Performance analysis of a new design of office diffuse ceiling ventilation system, Energy Build. 59 (2013) 73–81, https://doi.org/10.1016/j.enbuild.2013.01.001. ISSN 3787788, doi:10.1016/j.enbuild.2013.01.001.

[30] S. Petersen, N.U. Christensen, C. Heinsen, A.S. Hansen, Investigation of the displacement effect of a diffuse ceiling ventilation system, Energy Build. 85 (2014) 265–274, https://doi.org/10.1016/j.enbuild.2014.09.041. ISSN 3787788, doi:10.1016/j.enbuild.2014.09.041.

[31] T. Mikeska, J. Fan, Full scale measurements and CFD simulations of diffuse ceiling inlet for ventilation and cooling of densely occupied rooms, Energy Build. 107 (2015) 59–67, https://doi.org/10.1016/j.enbuild.2015.06.070. ISSN 3787788, doi:10.1016/j.enbuild.2015.06.070, https://linkinghub.elsevier.com/retrieve/pii/S0378778815301110.

[32] T. Yu, P.K. Heiselberg, B. Lei, M.Z. Pomianowski, C. Zhang, R.L. Jensen, Experimental investigation of cooling performance of a novel HVAC system combining natural ventilation with diffuse ceiling inlet and TABS, Energy Build. 105 (2015) 165–177, https://doi.org/10.1016/j.enbuild.2015.07.039. ISSN 3787788, https://linkinghub.elsevier.com/retrieve/pii/S0378778815301559.

[33] C. Zhang, T. Yu, P.K. Heiselberg, M.Z. Pomianowski, Experimental Study of an Integrated System with Diffuse Ceiling Ventilation and Thermally Activated Building Constructions, DCE Technical reports No. 182, Aalborg University, Aalborg, 2014.

[34] S. Terkildsen, S. Svendsen, Performance of low pressure mechanical ventilation concept with diffuse ceiling inlet for renovation of school classrooms, in: 32nd AIVC Conference and 1st TightVent Conference, 2011. Brussels, http://www.eceee.org/calendar/2011/AIVC.

[35] C. A. Hviid, S. Terkildsen, Experimental study of diffuse ceiling ventilation in classroom, 33rd AIVC conference, 2nd TightVent Conference .

[36] C. Zhang, M.H. Kristensen, J.S. Jensen, P.K. Heiselberg, R.L. Jensen, M. Pomianowski, Parametrical analysis on the diffuse ceiling ventilation by experimental and numerical studies, Energy Build. 111 (2016) 87–97, https://doi.org/10.1016/j.enbuild.2015.11.041. ISSN 3787788, doi:10.1016/j.enbuild.2015.11.041, https://linkinghub.elsevier.com/retrieve/pii/S0378778815304072.

[37] M.H. Kristensen, J.S. Jensen, P.K. Heiselberg, Field study evaluation of diffuse ceiling ventilation in classroom during real operating conditions, Energy Build. 138 (2017) 26–34, https://doi.org/10.1016/j.enbuild.2016.12.017. ISSN 3787788, doi:10.1016/j.enbuild.2016.12.017.

[38] T.E. Jiru, Y.-X. Tao, F. Haghighat, Airflow and heat transfer in double skin facades, Energy Build. 43 (10) (2011) 2760–2766, https://doi.org/10.1016/j.enbuild.2011.06.038. ISSN 3787788, https://linkinghub.elsevier.com/retrieve/pii/S0378778811002878.

[39] M. Hernandez Tascon, Experimental and Computational Evaluation of Thermal Performance and Overheating in Double Skin Facades, Ph.D. thesis, University of Nottingham, 2008, http://eprints.nottingham.ac.uk/10628/.

[40] A. Pappas, Z. Zhai, Numerical investigation on thermal performance and correlations of double skin façade with buoyancy-driven airflow, Energy Build. 40 (4) (2008) 466–475, https://doi.org/10.1016/j.enbuild.2007.04.002. ISSN 3787788, https://linkinghub.elsevier.com/retrieve/pii/S0378778807001181.

[41] E. Sanchez, A. Rolando, R. Sant, L. Ayuso, Influence of natural ventilation due to buoyancy and heat transfer in the energy efficiency of a double skin facade building, Energy Sustain. Dev. 33 (2016) 139–148, https://doi.org/10.1016/j.esd.2016.02.002. ISSN 9730826, https://linkinghub.elsevier.com/retrieve/pii/S0973082616000053.

[42] J. Joe, W. Choi, Y. Kwak, J.-H. Huh, Optimal design of a multi-story double skin facade, Energy Build. 76 (2014) 143–150, https://doi.org/10.1016/j.enbuild.2014.03.002. ISSN 3787788, doi:10.1016/j.enbuild.2014.03.002, https://linkinghub.elsevier.com/retrieve/pii/S0378778814001947.

[43] CEN, EN 16798-1, Energy Performance of Buildings—Ventilation for Buildings—Part 1: Indoor Environmental Input Parameters for Design and Assessment of Energy Performance of Buildings Addressing Indoor Air Quality, 2019.

[44] L. Karlsen, P.K. Heiselberg, I. Bryn, H. Johra, Solar shading control strategy for office buildings in cold climate, Energy Build. 118 (2016) 316–328, https://doi.org/10.1016/j.enbuild.2016.03.014. ISSN 3787788, https://linkinghub.elsevier.com/retrieve/pii/S0378778816301517.

[45] O. Mørck, A. Paulsen, S. Stiger, H. Erhorn-Kluttig, H. Erhorn, M. Zinzi, K. Buvik, K.E. Thomsen, Screening of Energy Renovation Measures for Schools – Denmark: school of the Future Towards Zero Emission with High Performance Indoor Environment, Tech. Rep, 2014, https://www.school-of-the-future.eu/images/files/20140124_SotF_Denmark.pdf.

[46] Verband Fenster + Fassade, Produktentwicklung und Produktdatenblätter - Fenster und Glas im Bestand, Tech. Rep, Verband Fenster + Fassade, Frankfurt am Main, 2008.

[47] Energistyrelsen, Bilag til Håndbog for Energikonsulenter 2006, 2006. Retrieved: 2020-12-03, http://www.hbemo.dk/sites/energihaandbog.dk/files/media/documents/hb2006/bilag-til-haandbog-for-energikonsulenter-2006.pdf.

[48] OECD, Education at a Glance 2020, Education at a Glance, OECD, 2020, https://doi.org/10.1787/69096873-en. ISBN 9789264382619, https://www.oecd-ilibrary.org/education/education-at-a-glance-2020_69096873-en.

[49] D. Teli, M.F. Jentsch, P.A. James, Naturally ventilated classrooms: an assessment of existing comfort models for predicting the thermal sensation and preference of primary school children, Energy Build. 53 (2012) 166–182, https://doi.org/10.1016/j.enbuild.2012.06.022. ISSN 3787788, https://linkinghub.elsevier.com/retrieve/pii/S0378778812003106.

[50] S.t. Mors, J.L. Hensen, M.G. Loomans, A.C. Boerstra, Adaptive thermal comfort in primary school classrooms: creating and validating PMV-based comfort charts, Build. Environ. 46 (12) (2011) 2454–2461, https://doi.org/10.1016/j.buildenv.2011.05.025. ISSN 3601323, https://linkinghub.elsevier.com/retrieve/pii/S0360132311001855.

[51] M. Havgaard Vorre, M. Hulmose Wagner, S.E. Maagaard, P. Noyé, N. Lynge, Branchevejledning for Indeklimaberegning, Statens Byggeforskningsinstitut, København, 2 edn., vol. 1, 2017. ISBN 9788756318501.

[52] T. Taylor, ICT Equipment Heat Gains Calculator - Excel Workbook, Retrieved: 29.01.2021, 2018, https://www.gov.uk/government/publications/classvent-and-classcool-school-ventilation-design-tool.

[53] CEN, CEN/TR 16798-2, Energy Performance of Buildings – Ventilation for Buildings – Part 2: Interpretation of the Requirements in EN 16798-1 – Indoor Environmental Input Parameters for Design and Assessment of Energy Performance of Buildings Addressing Indoor Air Quality, Thermal Environment, lighting and acoustics, 2019.
[54] CEN, EN 12464-1, Light and Lighting – Lighting of Work Places – Part 1: Indoor Work Places, 2011.
[55] Saint-Gobain Glass, Saint-Gobain Glass, 2020. Retrieved: 30.01.2021, https://de.saint-gobain-building-glass.com/de.
[56] L. Nippon, Sheet Glass Co., Pilkington, 2021. Retrieved: 30.02.2021, https://www.pilkington.com/.
[57] CEN, EN 673, Glass in Building – Determination of Thermal Transmittance (U value) – Calculation method, 2011.
[58] CEN, EN 410, Glass in Building – Determination of Luminous and Solar Characteristics of Glazing, 2011.
[59] International Energy Agency, Lighting, Tech. Rep, International Energy Agency, Paris, 2020, https://www.iea.org/reports/lighting.
[60] K. Pagh Nielsen, 2001 - 2010 Danish Design Reference Year - Update and Supplementary Datasets, DMI Report 18-20, Danish Meteorological Institute, 2018. https://www.dmi.dk/fileadmin/Rapporter/2018/DMI_report_18-20.pdf.
[61] O. Kalyanova, P.K. Heiselberg, Empirical Validation of Building Simulation Software: Modelling of Double Facades - Final Report, DCE Technical reports No. 27, Aalborg, 2009.
[62] E. Catto Lucchino, F. Goia, G. Lobaccaro, G. Chaudhary, Modelling of double skin facades in whole-building energy simulation tools: a review of current practices and possibilities for future developments, Build. Simulat. 12 (1) (2019) 3–27, https://doi.org/10.1007/s12273-019-0511-y. ISSN 1996-3599, http://link.springer.com/10.1007/s12273-019-0511-y.
[63] D.W. Kim, C.S. Park, Difficulties and limitations in performance simulation of a double skin façade with EnergyPlus, Energy Build. 43 (12) (2011) 3635–3645, https://doi.org/10.1016/j.enbuild.2011.09.038. ISSN 3787788.
[64] N.M. Mateus, A. Pinto, G.C.d. Graça, Validation of EnergyPlus thermal simulation of a double skin naturally and mechanically ventilated test cell, Energy Build. 75 (2014) 511–522, https://doi.org/10.1016/j.enbuild.2014.02.043. ISSN 3787788, https://linkinghub.elsevier.com/retrieve/pii/S0378778814001571.
[65] M. R. Krusaa, C. A. Hviid, Combining suspended radiant ceiling with diffuse ventilation – numerical performance analysis of low-energy office space in a temperate climate, J. Build. Eng. 38, ISSN 23527102, doi:10.1016/j.jobe.2021.102161, URL https://linkinghub.elsevier.com/retrieve/pii/S2352710221000176.
[66] C.A. Hviid, J. Lessing, Experimental study of the heat transfers and passive cooling potential of a ventilated plenum designed for uniform air distribution, in: CLIMA 2016 - Proceedings of the 12th REHVA World Congress, Aalborg, 2016.
[67] C.A. Hviid, S. Petersen, Integrated ventilation and night cooling in classrooms with diffuse ceiling ventilation, in: Ökosan '11, Graz, 2011.